Geochemistry Geophysics Geosystems G3

Article
Volume 14, Number 4
30 April 2013
doi:10.1002/ggge.20095
ISSN: 1525-2027

Published by AGU and the Geochemical Society

Confounding effects of coral growth and high SST variability on skeletal Sr/Ca: Implications for coral paleothermometry

Craig A. Grove and Geert-Jan A. Brummer
Department of Marine Geology, Royal Netherlands Institute for Sea Research (NIOZ), Texel, Netherlands (craig.grove@nioz.nl)

Sebastian Kasper
Department of Marine Geology, Royal Netherlands Institute for Sea Research (NIOZ), Texel, Netherlands

RWTH Aachen, Geologisches Institut, Aachen, Germany

Jens Zinke
Department of Marine Geology, Royal Netherlands Institute for Sea Research (NIOZ), Texel, Netherlands

School of Earth and Environment, The University of Western Australia and the UWA Oceans Institute, Crawley WA, Australia and the Australian Institute of Marine Science, Nedlands WA, Australia

Miriam Pfeiffer
RWTH Aachen, Geologisches Institut, Aachen, Germany

Dieter Garbe-Schönberg
University of Kiel, Institut für Geowissenschaften, Kiel, Germany

[1] Massive corals offer continuous records of climate locked within their skeleton, with the most commonly applied paleo-thermometer being Sr/Ca. Recently, however, problems with Sr/Ca thermometry indicate that the intrinsic variance of single-core Sr/Ca time series differs between cores. Here, we compare the Sr/Ca records and growth parameters of two *Porites lutea* colonies sampled from the same reef zone, 0.72 km apart, with two gridded SST datasets, ERSST and HadISST, off NE Madagascar. Specifically, we address seasonal and interannual variability as well as trend differences between records over the same 43 year period. The two gridded SST datasets showed strong seasonality and weak positive ENSO anomalies on a slow 43 year warming trend at significantly different rates. Both the coral Sr/Ca records showed the same clear seasonality and similar amplitudes in SST. However, on interannual timescales, they displayed diverging 43 year Sr/Ca trends and opposite responses to weak ENSO anomalies. Moreover, their growth response also differed as one coral showed increasing extension/calcification rates and Sr/Ca ratios (cooling) over the 43 years, while the other coral showed decreasing extension/calcification rates and Sr/Ca ratios (warming). Further, during positive ENSO events, the calcification rates of the two corals were negatively correlated, while skeletal density anomalies were opposite. Possible explanations to why these corals are so different may be related to the corals growth response to SST changes. The growth response of individual corals to increasing SST seems to be opposite, which in turn are likely related to biological factors. Consequently, coral growth responses explain much of the inter-colony Sr/Ca variability.

Components: 9,800 words, 8 figures, 4 tables.

Keywords: coral; Sr/Ca; SST; growth; ENSO; vital effect.

Index Terms: 4916 Paleoceanography: Corals (4220); 4954 Paleoceanography: Sea surface temperature; 4922 Paleoceanography: El Nino (4522).

Received 9 October 2012; **Revised** 11 February 2013; **Accepted** 13 February 2013; **Published** 30 April 2013.

Grove, C. A., S. Kasper, J. Zinke, M. Pfeiffer, D. Garbe-Schönberg, and G.-J. A. Brummer (2013), Confounding effects of coral growth and high SST variability on skeletal Sr/Ca: Implications for coral paleothermometry, *Geochem. Geophys. Geosyst.*, *14*, 1277–1293, doi:10.1002/ggge.20095.

1. Introduction

1.1. Coral Paleothermometry

[2] Massive corals, such as *Porites* spp., can grow for centuries while residing in a fixed position, continuously building an aragonite ($CaCO_3$) skeleton at a rate between 0.5 and 2 cm yr^{-1}. As the coral precipitates its skeleton, a number of minor and trace elements are incorporated at different concentrations, relative to Ca, in relation to changing physiochemical parameters [*Felis and Pätzold*, 2003]. The Sr/Ca ratio of the coral aragonite seems to be the most applied paleo-thermometer, whereby a negative relationship exists with SST, i.e., as temperatures increase, less Sr is incorporated into the aragonite lattice relative to Ca [*Alibert and McCulloch*, 1997; *DeLong et al.*, 2007]. A compilation of Sr/Ca-SST calibrations for *Porites* spp. revealed a mean Sr/Ca relationship with SST of −0.061mmol/mol per 1°C increase [*Corrège*, 2006]. Since Sr has a long oceanic residence time, heterogeneity in skeletal Sr/Ca is assumed to mainly reflect SST variability. Therefore, down-core sampling of massive corals yields an in situ SST time series in which the resolution is only limited by the coral growth rate.

[3] Coral skeletal Sr/Ca heterogeneity has been found to not only reflect temperature variability. Micro-analytical studies have shown the distribution of Sr to be highly heterogeneous at the micrometer scale, corresponding to skeletal components and ultra-structure [*Allison*, 1996; *Cohen et al.*, 2002]. Consequently, sampling along calcification centers should be avoided where Sr/Ca are relatively high [*Hart and Cohen*, 1996; *Alibert and McCulloch*, 1997; *Gaetani and Cohen*, 2006; *DeLong et al.*, 2007]. Other biological factors, or "vital effects", are also thought to influence Sr concentrations in the skeleton. Changing extension rate and density of the corals, associated with calcification processes (vital effect), have been shown to correlate with Sr/Ca [*de Villiers et al.*, 1994; *Alibert and McCulloch*, 1997; *Allisonl*, 1996; *Allison et al.*, 2001; *Ferrier-Pages et al.*, 2002; *Sinclair*, 2005; *Sinclair et al.*, 2006; Saenger *et al.*, 2008; *Cohen and Gaetani*, 2010; *Kuffner et al.*, 2012]. Complicating the relationship further, some studies have found that temperature itself is influencing growth parameters such as coral extension rates [*Lough and Barnes*, 2000; *Cantin et al.*, 2010; *Storz and Gischler*, 2011]. This in turn may indirectly influence the Sr/Ca signal.

[4] Recently, published coral Sr/Ca records covering the past hundreds of years indicate specific problems with the Sr/Ca thermometer, particularly on decadal to secular time scales [e.g., *Linsley et al.*, 2004, 2006; *Quinn et al.*, 2006]. *Pfeiffer et al.* [2009] showed that the intrinsic variance of the single-core Sr/Ca time series differs from core to core, limiting their use for absolute estimates of past temperature variations. This inter-colony variability seems linked to vital effects. Averaging the multiple-core data improves the correlation with instrumental temperature and allows more accurate estimates of interannual temperature variations (0.35°C or better) [*Pfeiffer et al.*, 2009]. Here, we assess the reproducibility of SST reconstructions from two northeast Madagascar coral Sr/Ca records, located 0.72 km apart. We argue that single-core Sr/Ca records are modulated by changes in the colony growth response to temperature, which may overwhelm the actual SST signal in the skeleton [*Cohen and Gaetani*, 2010; *Gaetani et al.*, 2011]. To test this, we examine the inter-colony skeletal Sr/Ca and growth variability of two corals over the same 43 year period and compare our results with gridded SST for the region.

1.2. Historical SST Data

[5] The assessment of site-specific reef environments to temperature change is largely based on the analyses of long-term gridded instrumental SST data [e.g., *McClanahan et al.*, 2009]. This form of data averages large areas (1°×1° or 2°×2°) with often few in situ measurements, therefore reef scale

interannual variability associated with ENSO and long-term SST trends may be underestimated. Indeed, our study site in northeast Madagascar has little or no historical in situ SST observations (ICOADS SST data) [*Woodruff et al.*, 2005], making it difficult to assess the validity of skeletal Sr/Ca as a reef-scale paleothermometer. For this reason, we use and compare two gridded SST datasets to evaluate relative regional trends and interannual variability and compare with coral Sr/Ca-based SST variability.

[6] Historical SST data collected primarily by ships-of-opportunity has been summarized in the comprehensive ocean atmosphere dataset (ICOADS) to produce monthly averages on a 2°×2° grid basis [*Woodruff et al.*, 2005]. In the grid that includes the island of St. Marie (northeast Madagascar), the data are extremely sparse (http://climexp.knmi.nl). We therefore extracted SST from the extended reconstructed SST (ERSST) version 3 [*Smith and Reynolds*, 2004], also based on ICOADS data, which uses sophisticated statistical methods to reconstruct SST in times of sparse data. From ERSST, we extracted data in the 2°×2° grid centered at 49–50°E, 17–18°S. Over the period 1963 to 2006, the ERSST data averaged 26.31°C (± 1.60°C), with an average annual range of 5.61°C (Table 1).

[7] In addition to ERSST, we used Met Office Hadley Center's sea ice and sea surface temperature (HadISST) data for the grid 49–50°E, 17–18°S [*Rayner et al.*, 2003]. HadISST temperatures are reconstructed using a two-stage reduced-space optimal interpolation procedure, followed by superposition of quality-improved gridded observations onto the reconstructions to restore local detail. Since January 1982, SST time series for HadISST use the optimal interpolation SST, version 2 [*Reynolds et al.*, 2002] that includes continuous time series of satellite-based SST measurements. Over the period 1963 to 2006, the HadISST data averaged 26.48°C (± 1.58°C), with an average annual range of 5.62°C (Table 1).

Table 1. Statistical Comparison of ERSST and HadISST for the Same Study Site (49º–50ºE – 17º–18ºS) Based on Monthly Replicated 100 × 100 km Data for the Years Between 1963 and 2006

Variable	ERSST v.3b2 SST 49º–50ºE, 17º–18ºS	HadISST 49º–50ºE, 17º–18ºS
Mean	26.31	26.48
Standard error	0.07	0.07
Median	26.24	26.68
Mode	28.16	28.03
Standard deviation	1.60	1.58
Sample variance	2.56	2.50
Kurtosis	−1.44	−1.41
Skewness	−0.09	−0.19
Range	5.61	5.62
Minimum	23.29	23.56
Maximum	28.90	29.18
Sum	13,601.54	13,690.47
Count	517.00	517.00
SST rise ($Cyr^{\wedge-1}$)	0.010	0.002

[8] Recent analysis of several gridded SST products showed that important differences exist in long-term SST trends [*Solomon and Newman*, 2012]. For the entire 1963 to 2006 time series, ERSST and HadISST displayed slight statistical differences, with the major exception being a twofold difference in the skewness of the data (Table 1). Consequently, the 43 year trend from 1963 to 2006 in ERSST and HadISST differs, being 0.010°C yr^{-1} and 0.002°C yr^{-1}, respectively (Table 1). Indeed, *Solomon and Newman* [2012] showed that grid-based warming trends in the SW Indian Ocean are uncertain, as some grid products show significant warming, while others do not. Nevertheless, given both grid-based datasets show positive trends, we assume some degree of warming has occurred in the region over the 43 year period and will test whether our corals record this in their skeletal Sr/Ca records.

[9] During a positive El Niño-Southern Oscillation (ENSO) event, the southwest Indian Ocean, including our study site, experiences small positive SST anomalies during the mature ENSO phase between January and March (JFM; Figure S1, Supporting Information)[1], [*Schott et al.*, 2009]. The 12 El Niño events (defined by the Oceanic Niño Index/ONI; www.cpc.ncep.noaa.gov) that occurred between the period 1963 and 2006 (1966, 1969, 1973, 1977, 1983, 1987, 1988, 1992, 1995, 1998, 2003, 2005) lead to minor, variable warming around the St. Marie region of 0.22°C (±0.23°C) and 0.25°C (±0.23°C), calculated over a 3 month average from January to March according to ERSST and HadISST, respectively (JFM_{ENSO} - JFM_{tot}; Table S1). The magnitude of these SST anomalies are small and therefore lie within the range of observational errors [*Annamalai et al.*, 1999], potentially resulting in a poor signal-to-noise ratio of Indian Ocean grid SST. Nevertheless, HadISST and ERSST show more or less consistent ENSO-related mean SST anomalies; therefore, the signature appears to be more robust with respect to linear trends.

[1]Additional Supporting Information may be found in the online version of this article.

2. Materials and Methods

2.1. Coral Sampling

[10] In March 2007, coral cores STM2 and STM4 were drilled from two separate massive dome-shaped colonies of *Porites lutea* on the eastern side of St. Marie, an island off the East coast of Madagascar, facing the open SW Indian Ocean (Figure 1). Colony STM4 measured 4.5 m in height and 3.5 m in diameter, while colony STM2 was 1.8 m in height with a diameter of 1.8 m. A commercially available pneumatic drill (Rodcraft 4500) was used to extract 4 cm diameter cores along the central growth axis of the colony. The apexes of the colonies were situated 1.0 m and 0.5 m below the water surface at low tide for STM2 and STM4, respectively (Table 2). Colonies were located 0.72 km from each other, growing in coral sand patches in the back reef of a fringing reef and experiencing good exchange with oceanic waters (Figure 1; Table 2). The total length of cores STM2 and STM4 were 180 cm and 365 cm, respectively.

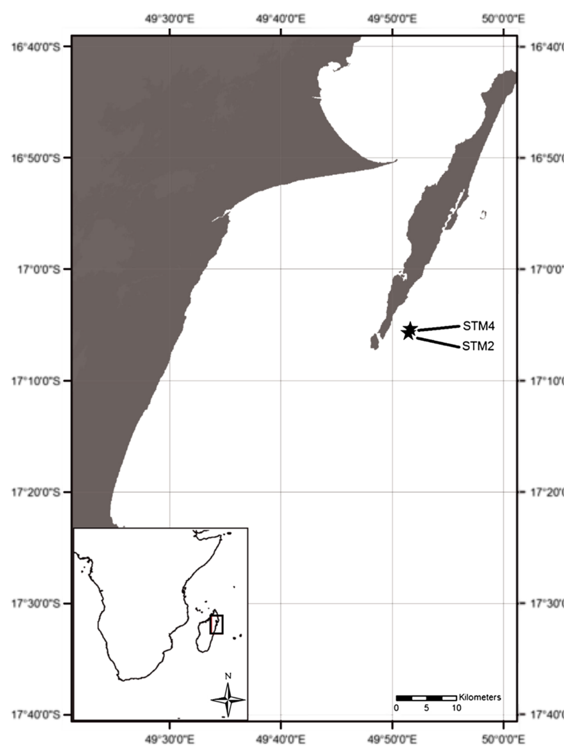

Figure 1. Location of coral cores STM2 and STM4 (stars) off the eastern coast of St. Marie, NE Madagascar (bottom left). The coral cores are located 0.72 km apart.

[11] Coral cores were sectioned lengthwise into equal 7 mm thick slabs, rinsed several times with demineralized water, blown with compressed air to remove any surficial particles and dried for more than 24 h in a laminar flow hood. Annual bands were visualized by X-radiograph-positive prints and luminescence imagery [*Hendy and Gagan*, 2003; *Grove et al.*, 2010]. As there is no humic acid input from terrestrial sources, the intensity of luminescence is considered to be a product of density only [*Barnes and Taylor*, 2005; *Grove et al.*, 2010]. Visualizing the growth axis of the coral slab meant we could define the sampling track perpendicular to the bands (Figures S2 and S3). Unfortunately, it was difficult to distinguish between the individual corallite bundles of STM4; therefore, the sampling track may be slightly offset to the optimal growth axis for the years before 1978 (Figure S3). Using a diamond coated drill of 1.1 mm in diameter, subsamples for Sr/Ca analysis were taken every 1 mm parallel to the growth axis, equivalent to an approximate monthly resolution. Both datasets cover the same 43 year period of 1963 to 2006. The annual extension rates (cm yr^{-1}) were calculated by measuring the distance (cm) between Sr/Ca maxima. Coral densities (g/cm^3) were calculated by analyzing digital X-rays using the program CoralXDS [*Helmle et al.*, 2002; *Carricart-Ganivet et al.*, 2007; *Helmle et al.*, 2011], and calcification rate (g/cm^2 yr^{-1}) by multiplying density with extension rate.

2.2. Analytical Procedures

[12] Skeletal Sr/Ca sub-samples were measured by inductively coupled plasma optical emission spectrometry (ICP-OES) using a simultaneous, radially viewing instrument (Ciros side-on plasma, SPECTRO Analytical Instruments GmbH, Kleve, Germany) at the University of Kiel. Respective element emission signals were simultaneously collected

Table 2. Coral Core Names Listed Together With Their GPS Coordinates, Depths at Low Tide, and Mean Rates of Extension, Calcification, and Densities Over the Same 43 Year Period

Core name	GPS Position	Species	Water Depth (m)	Mean Growth Rate cm yr^{-1}	Mean Density g/cm^3	Mean Calcification Rate g/cm^2 yr^{-1}
STM2	S17º05.685 E49º51.483	*Porites lutea*	1.0	1.42 (±0.22)	0.86 (±0.13)	1.21(±0.24)
STM4	S17º05.322 E49º51.632	*Porites lutea*	0.5	1.79 (±0.35)	0.65 (±0.03)	1.15(±0.21)

and subsequently drift corrected by sample-standard bracketing every 10 samples following a combination of techniques described by *Schrag* [1999] and *de Villiers et al.* [2002]. The sample solution was prepared by dissolving approximately 0.5 mg of coral powder in 1.00 ml ultrapure HNO_3 2%. The working solution was prepared by serial dilutions of the sample solution with HNO_3 2% to a Ca concentration of ca. 8 ppm. Standard solution was prepared by diluting 1.00 ml of the stock solution (0.52 grams of homogenized coral powder from an in-house standard in 250 ml HNO_3 2%) with 2.00 ml ultrapure HNO_3 2%. The Sr and Ca lines used for this measurement were 407 and 317 nm, respectively. Analytical precision on Sr/Ca determinations was 0.15% RSD or 0.01 mmol/mol (1σ). Over the entire measurement period of 2 weeks, the average Sr/Ca of the JCp_1 standard [*Inoue et al.*, 2004] was 8.57 mmol/mol, with a RSD of 0.09 %.

2.3. Coral Chronology

[13] The coral chronologies were developed based on the seasonal cycle of Sr/Ca (Figure 2) and corroborated against luminescence and X-ray density profiles. We assigned the coldest month (either August or September) to the highest measured Sr/Ca ratio in any given year, according to both HadISST and ERSST. We then interpolated linearly between these anchor points to obtain age assignments for all other Sr/Ca measurements. In a second step, the Sr/Ca data was interpolated to 12 equidistant points per year to obtain monthly time series using AnalySeries 2.0 [*Paillard et al.*, 1996]. This approach creates a non-cumulative time scale error of 1–2 month in any given year due to interannual differences in the exact timing of peak SST. The monthly resolved age model for density was created by aligning the X-ray density profile with the Sr/Ca based age model.

3. Results

3.1. Single and Composite Sr/Ca Records

[14] Both STM2 and STM4 showed strong seasonal cycles in the monthly Sr/Ca time series (Figure 2). Also, $STM_{composite}$ shows clear seasonality in monthly Sr/Ca with a mean value of 8.868 mmol/

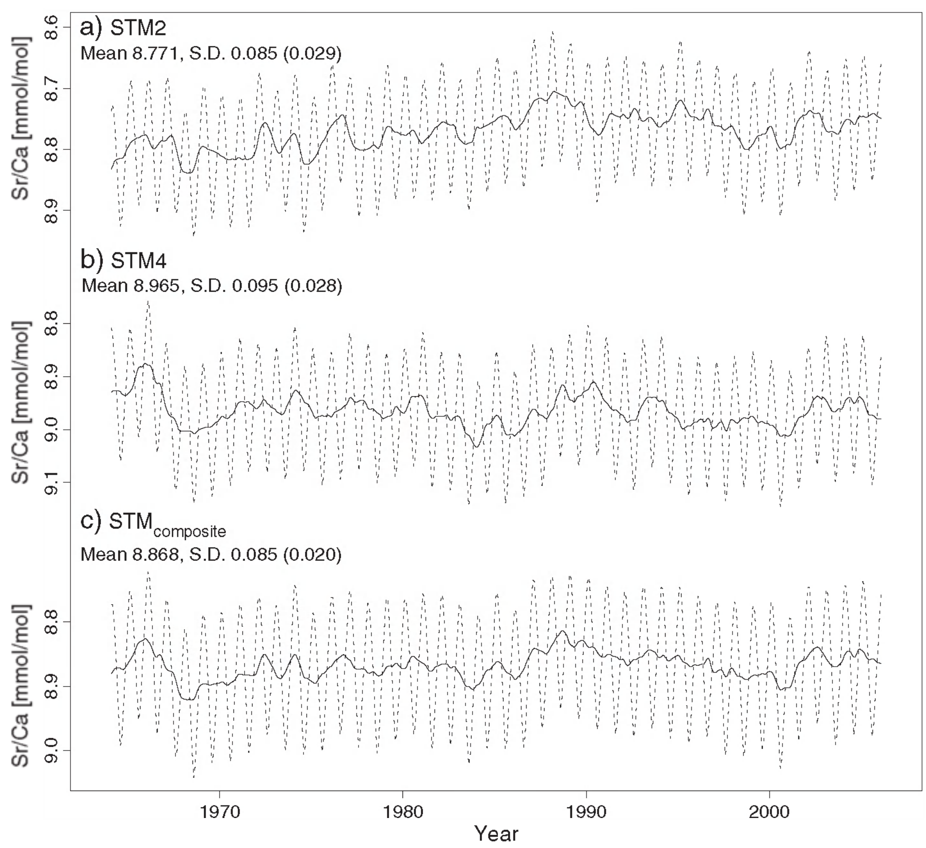

Figure 2. Monthly interpolated Sr/Ca time series (dotted line) and 12 month moving average (solid line) of coral cores (a) STM2, (b) STM4, and (c) the $STM_{composite}$. Means and standard deviations of monthly (annual mean) time series are indicated above left of the corresponding core record.

Table 3. Linear Regression Equations, Correlation Coefficients, and Significance Levels of Monthly, Annual Mean and Max-min Sr/Ca with both ERSST (gray) and HadISST (White) for STM2, STM4, and $STM_{composite}$[a]

Monthly[a]	Regression equation	r^2	P	σ[b]
STM4	Sr/Ca = -0.051(±0.001) * SST + 10.304 (±0.036)	0.732	$< 2.2*10^{-16}$	0.05
	Sr/Ca = -0.052(±0.001) * SST + 10.338(±0.036)	0.741	$< 2.2*10^{-16}$	0.05
STM2	Sr/Ca = -0.045(±0.001) * SST + 9.951(±0.032)	0.721	$< 2.2*10^{-16}$	0.04
	Sr/Ca = -0.045(±0.001) * SST + 9.963(±0.048)	0.710	$< 2.2*10^{-16}$	0.05
$STM_{composite}$	Sr/Ca = -0.048(±0.001) * SST + 10.127(±0.026)	0.820	$< 2.2*10^{-16}$	0.04
	Sr/Ca = -0.048(±0.001) * SST + 10.151(±0.027)	0.819	$< 2.2*10^{-16}$	0.04

Annual mean[a]	Regression equation	r^2	P	σ[b]
STM4	Sr/Ca = -0.013(±0.019) * SST + 8.624 (±0.509)	0.011	0.506	0.03
	Sr/Ca = -0.002(±0.021) * SST + 9.020(±0.036)	0.0002	0.923	0.03
STM2	Sr/Ca = -0.056(±0.018) * SST + 10.245(±0.474)	0.191	0.003	0.03
	Sr/Ca = -0.030(±0.021) * SST + 9.555(±0.567)	0.045	0.174	0.03
$STM_{composite}$	Sr/Ca = -0.022(±0.013) * SST + 9.434(±0.353)	0.059	0.116	0.02
	Sr/Ca = -0.016(±0.015) * SST + 9.287(±0.395)	0.027	0.295	0.02

Max-min[a]	Regression equation	r^2	P	σ[b]
STM4	Sr/Ca = -0.064(±0.002) * SST + 10.640(±0.057)	0.909	$< 2.2*10^{-16}$	0.04
	Sr/Ca = -0.064(±0.002) * SST + 10.664(±0.055)	0.919	$< 2.2*10^{-16}$	0.04
STM2	Sr/Ca = -0.055(±0.002) * SST + 10.204(±0.046)	0.920	$< 2.2*10^{-16}$	0.04
	Sr/Ca = -0.055(±0.002) * SST + 10.211(±0.048)	0.912	$< 2.2*10^{-16}$	0.04
$STM_{composite}$	Sr/Ca = -0.057(±0.001) * SST + 10.379(±0.035)	0.956	$< 2.2*10^{-16}$	0.03
	Sr/Ca = -0.058(±0.001) * SST + 10.392(±0.035)	0.956	$< 2.2*10^{-16}$	0.03

[a]ERSST and HadISST data are from the region 49º–50ºE, 17º–18ºS for the years between 1963 and 2006.
[b]The residual standard errors are given as σ.

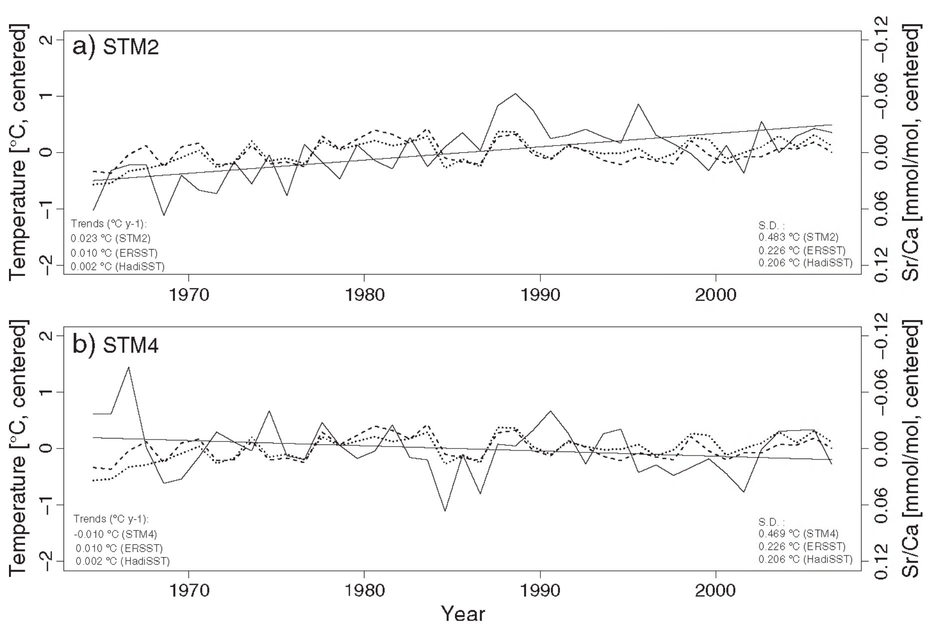

Figure 3. Annual mean Sr/Ca time series (solid line) of (a) STM2 and (b) STM4, together with the annual mean ERSST (dotted line) and HadISST (dashed line) time series. Sr/Ca has been scaled so that –0.06 mmol/mol corresponds to a warming of 1°C [*Corrège*, 2006]. The standard deviation and trends of all time series are given in the bottom right and left of each record, respectively. Linear trends are shown as a straight black line.

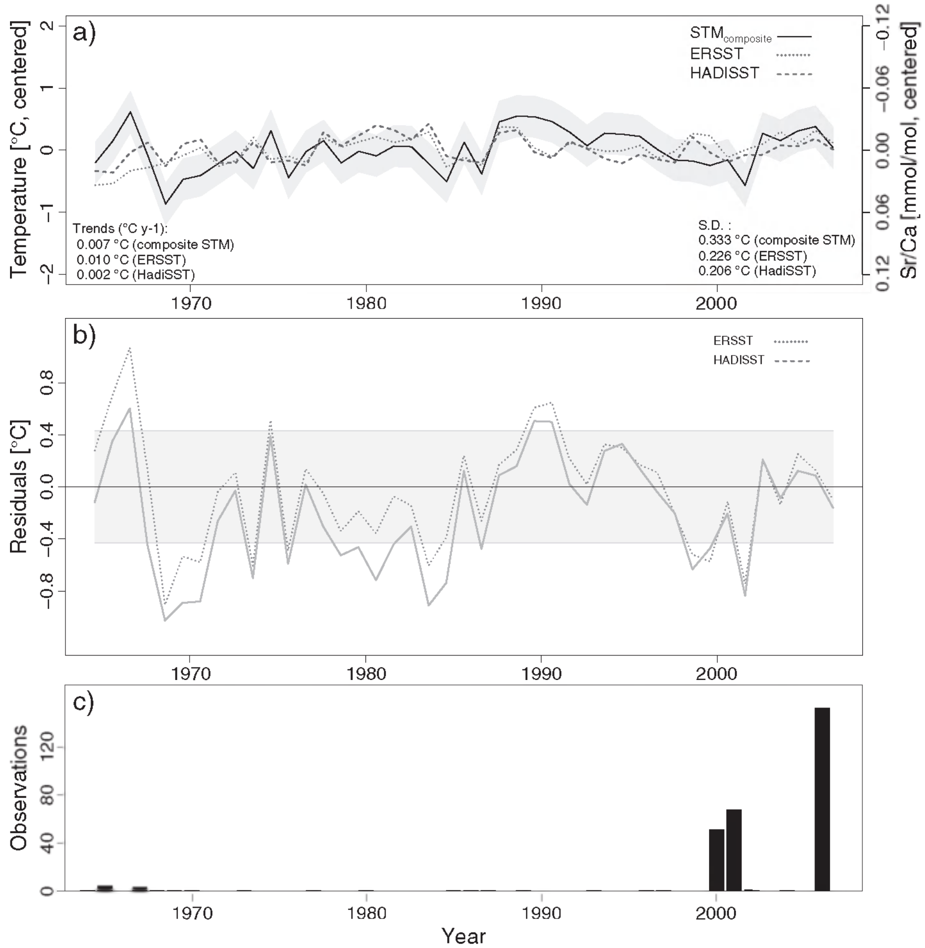

Figure 4. (a) Time series of annual mean composite Sr/Ca ($STM_{composite}$; solid line), ERSST (dotted line) and HadISST (dashed line), with trends and standard deviation (1σ) bottom right and left, respectively. Composite Sr/Ca is the arithmetic mean of STM2 and STM4, with $\pm$1 SD shaded. (b) Temperature residuals of ERSST (dotted line) and HadISST (dashed line) are shown in relation to $STM_{composite}$, with $\pm$1 SD shaded. Sr/Ca has been scaled so that -0.06 mmol/mol corresponds to 1°C. (c) The number of observations, according to ICOADS, is shown for the 43 years used for this study.

mol (Figure 2). The $STM_{composite}$ is the arithmetic mean of STM2 and STM4, which have statistically different 43 year means (>1σ) at 8.771 mmol/mol and 8.965 mmol/mol, respectively (Figure 2). The standard deviations (1σ) around the means of STM2 and $STM_{composite}$ were the same at 0.085 mmol/mol, whereas STM4 is slightly higher at 0.095 mmol/mol (Figure 2).

[15] Regressions of monthly Sr/Ca with gridded SST all gave very high correlation coefficients ($r^2 = 0.710 - 0.820$), enhanced by the seasonal cycles inflating relationships. Relationships were further enhanced when the maximum and minimum (max-min) Sr/Ca values were regressed against the coldest and warmest months in SST, respectively ($r^2 = 0.909 - 0.956$; Table 3). For both cores and the composite, the monthly and max-min slope relationship to a 1°C increase in ERSST and HadISST ranged between -0.064 mmol/mol°C^{-1} and -0.045 mmol/mol°C^{-1} (Table 3). These values are close to that of a recent compilation of Sr/Ca-SST calibrations [*Corrège*, 2006].

[16] The annual means of the three Sr/Ca records, STM2, STM4, and $STM_{composite}$, were calculated by averaging the Sr/Ca values for all months from September through to August, the two coldest months of the calendar year. The standard deviations for the annual means for STM2, STM4, and $STM_{composite}$ were 0.029 mmol/mol, 0.028 mmol/mol, and 0.020 mmol/mol, respectively (Figure 2). The correlation coefficient of the annual mean Sr/Ca for STM2 regressed against STM4 was not significant: $r^2 = 0.0004$, $n = 43$, $p = 0.9$. When only considering the recent period 1982 – 2006, the relationship was also not significant ($r^2 = 0.1$, $n = 25$, $p = 0.12$).

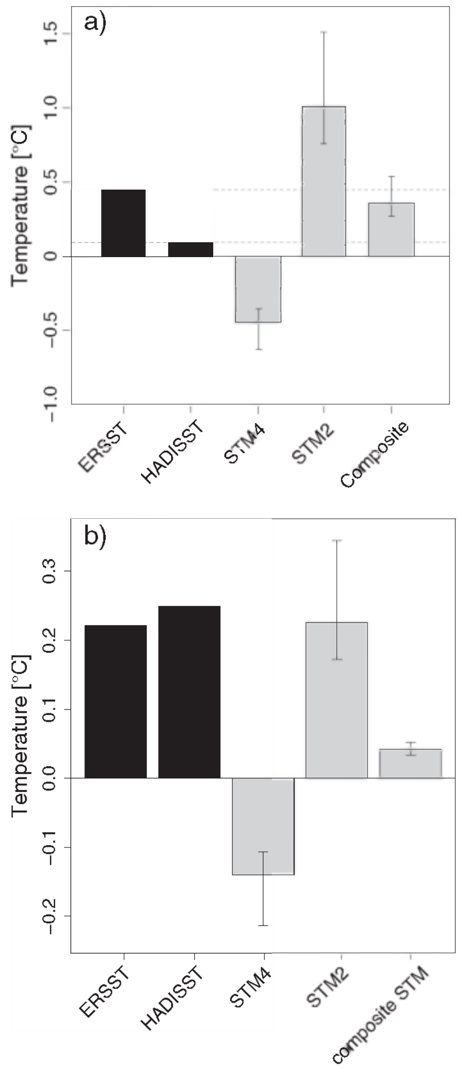

Figure 5. (a) The mean temperature change and (b) average ENSO anomalies for 12 positive ENSO years over the 43 year period used in this study (1963 – 2006) for ERSST and HadISST (black bars), and STM2, STM4, and $STM_{composite}$ (gray bars). ENSO anomalies were calculated by subtracting the mean JFM_{ENSO} SST (Sr/Ca) from the mean JFM_{tot} SST (Sr/Ca). Coral Sr/Ca was converted to temperature units using −0.06 mmol/mol/°C [*Corrège*, 2006]. Error bars on Sr/Ca temperatures are computed using the range of published slopes, being −0.04 and −0.08 mmol/mol/°C [*Corrège*, 2006].

[17] Linear regressions of the coral annual means against either ERSST or HadISST annual means (September-August) resulted in very low correlation coefficients with consistently negative slopes (Table 3). Only STM2 regressed against ERSST returned a correlation coefficient that was significant at the 95% confidence level, being $r^2 = 0.19$, $p < 0.005$ (Table 3). Its slope of −0.056 mmol/mol/°C is within the range of published relationships [*Corrège*, 2006] (Table 3). For STM4, removal of the anomalous warm years pre-1972 slightly improved correlations with ERSST (not HadISST) ($r^2 = 0.1$, $p < 0.07$), and its slope of −0.044 mmol/mol/°C falls within the lower range of published relationships [*Corrège*, 2006]. Detrending annual mean Sr/Ca and gridded data did not improve regressions for either STM2 or STM4. Further, the significant correlation of STM2 with gridded ERSST data was lost after detrending.

3.2. Trend Estimates

[18] Coral Sr/Ca was converted to relative temperature units using the relationship of −0.06 mmol/mol per 1°C warming [*Corrège*, 2006], which is close to the local relationships established above. We used this slope to treat both coral records equally and make results comparable. All 43 year SST trends were different, with ERSST showing a warming of 0.010°C yr^{-1} (+0.430°C trend), HadISST a slight warming of 0.002°C yr^{-1} (+0.086°C trend), STM2 a strong warming of 0.023°C yr^{-1} (+0.989°C trend), and STM4 a cooling of 0.010°C yr^{-1} (−0.430°C trend) (Figure 3). Despite diverging trends in STM2 and STM4, both showed similar standard deviations of 0.483°C and 0.469°C, respectively, about twice that of ERSST (0.226°C) and HadISST (0.206°C). The annual mean of the $STM_{composite}$ had a standard deviation of 0.333°C, less than STM2 and STM4 yet higher than ERSST and HadISST (Figure 4). The $STM_{composite}$ had a warming trend of 0.007°C yr^{-1} (+0.301°C trend over 43 years), which lies between the trends of the two gridded SST time series (Figures 4 and 5a). Figure 5a indicates the large discrepancies between the five trends, of which $STM_{composite}$ is shown to be outside both the error bars of STM2 and STM4. A direct comparison of the annual means of $STM_{composite}$ with the gridded SST data shows higher residuals (>1σ) in the earlier period that decrease towards present day (Figure 4). Further, for the years (2000, 2001, and 2006) with a large number of SST observations (ICOADS; Figure 4c), the differences between residuals were closer to zero.

3.3. ENSO Years

[19] According to ERSST and HadISST, the average SST anomaly for 12 ENSO years calculated over a 3 month average from January to March lead to warming of 0.22°C (±0.23°C) and 0.25°C (±0.23°C), respectively. Subtracting the mean

JFM_{ENSO} Sr/Ca from the mean JFM Sr/Ca for the same 12 years provides an estimate of the Sr/Ca ENSO anomaly recorded in each coral. Reconstructed ENSO-related SST anomalies were therefore calculated by subtracting the mean JFM_{ENSO} SST (Sr/Ca) from the mean JFM_{tot} SST (Sr/Ca). STM2 had a negative Sr/Ca anomaly of −0.014 mmol/mol (±0.037 mmol/mol), whereas STM4 had a positive anomaly of 0.009 mmol/mol (±0.029 mmol/mol; Table 4a). Coral Sr/Ca was then converted to temperature units using the relationship of −0.06 mmol/mol per 1°C warming [*Corrège*, 2006], which resulted in mean SST anomalies of 0.23°C (±0.61°C) and −0.14°C (±0.49°C) for STM2 and STM4, respectively (Figure 5b and Table S1). A two-sided t-test showed that the ENSO-related Sr/Ca-based SST anomalies for STM2 and STM4 were significantly different at the 10% confidence level ($p = 0.07$). The $STM_{composite}$ Sr/Ca anomaly was −0.003 mmol/mol (±0.024 mmol/mol; Table 4a), which equates to a mean warming of 0.04°C (±0.40°C) (Figure 5b and Table S1). The Sr/Ca difference between the STM4 and STM2 anomaly was negative at −0.005 mmol/mol (STM4-STM2), equating to a positive SST anomaly of 0.08°C.

[20] Assessing the individual positive ENSO events indicated that only STM2 showed reasonable agreement with instrumental SST data, compared to STM4 and $STM_{composite}$ (Table S1). Using a rank sum test, we compared the coral-based SST anomalies with ERSST and HadISST anomalies. For STM4 and $STM_{composite}$ anomalies, a significant difference in the median values was observed with both ERSST and HadISST anomalies (95% confidence level). Only the ENSO-related Sr/Ca based SST anomalies of STM2 were statistically similar to both sets of grid-based SST anomalies (95% confidence level).

3.4. Growth Parameters

[21] Annual coral extension rates showed diverging trends over the 43 years (Table 2), with STM2 declining by −0.007 cm yr^{-1} and STM4 increasing by +0.018 cm yr^{-1} (Figures 6 and 7). Neither corals showed a significant change during the 12 ENSO years compared to the 43 year mean in annual extension rates. The average ENSO year extension rate for STM2 was 1.41 cm yr^{-1} (±0.19 cm yr^{-1}) and 1.75 cm yr^{-1} (±0.35 cm yr^{-1}) for STM4 (Table 2).

Table 4. ENSO-related Sr/Ca and Skeletal Density Anomalies for STM2, STM4, and $STM_{composite}$

(a) Sr/Ca[a]	JFM_{ENSO} mmol/mol	JFM_{tot} mmol/mol	ENSO Anomaly[b]
STM2	8.671 (± 0.037)	8.685 (± 0.034)	−0.014 (± 0.037)
STM4	8.868 (± 0.029)	8.859 (± 0.031)	+0.009 (± 0.029)
$STM_{composite}$	8.769 (± 0.024)	8.772 (± 0.025)	−0.003 (± 0.024)
(b) Density[a]	JFM_{ENSO}	JFM_{tot}	ENSO anomaly
STM2	0.874 (± 0.121)	0.858 (± 0.121)	+0.016 (± 0.121)
STM4	0.638(± 0.028)	0.643 (± 0.034)	−0.005 (± 0.028)

[a]Anomalies were calculated by subtracting the mean Sr/Ca/density value for January to March (JFM) from the mean JFM Sr/Ca/density for the 12 ENSO years (1966, 1969, 1973, 1977, 1983, 1987, 1988, 1992, 1995, 1998, 2003, 2005) between 1963 and 2006.
[b]The net difference between the ENSO Sr/Ca anomaly of STM2 and STM4 equates to −0.005 mmol/mol.

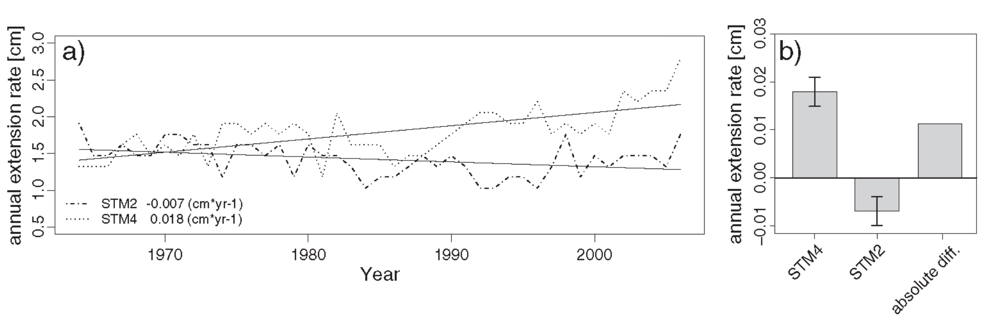

Figure 6. (a) The mean annual extension rates over the 43 year period (1963 – 2006) for STM2 (stippled line) and STM4 (dotted line) are shown together with linear trends (straight black lines). (b) The extension rate trend is also indicated (bottom left for both records) and shown graphically for STM2 and STM4, together with the trend difference (STM4-STM2). Error bars indicate the slope standard error.

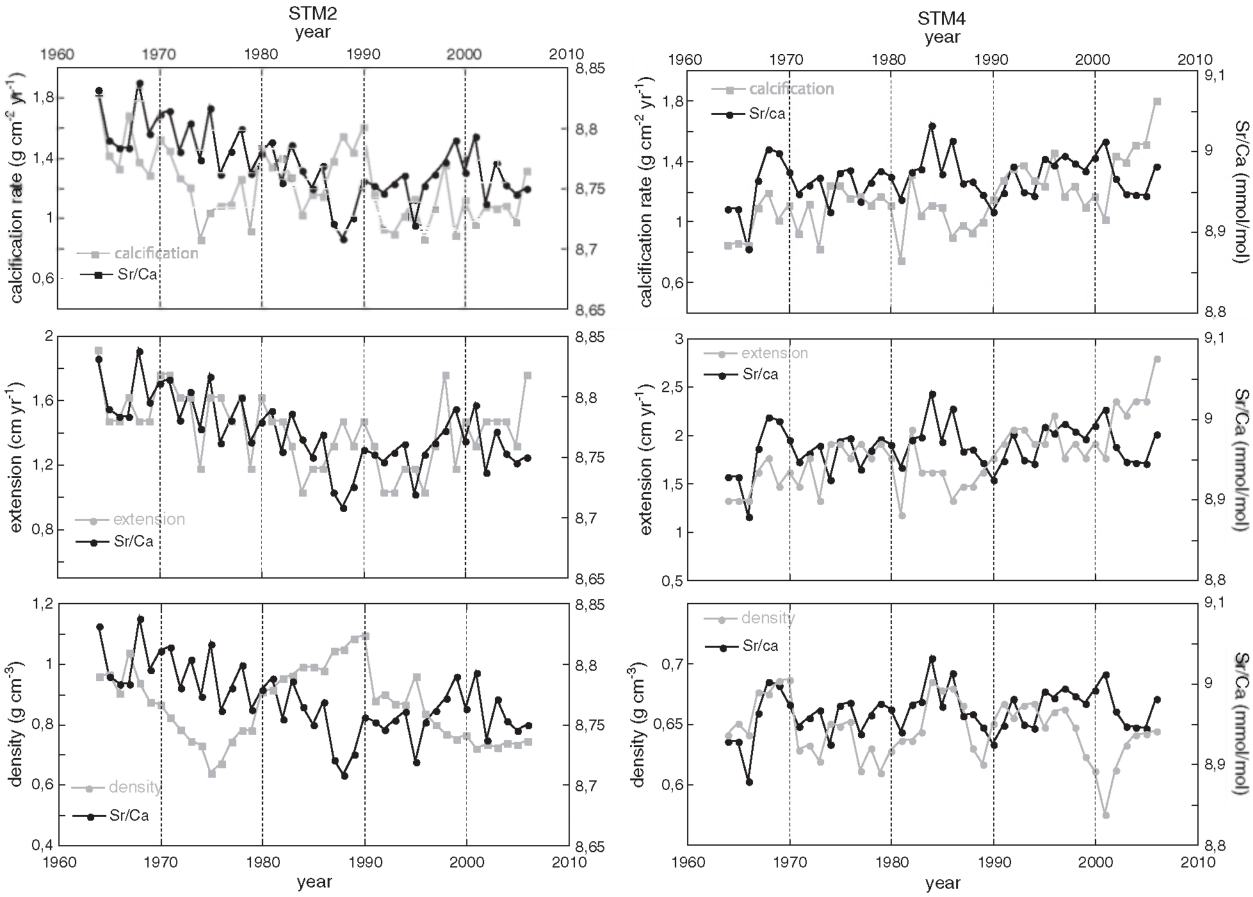

Figure 7. (Top) Time series of annual mean coral Sr/Ca ratios compared to calcification rate, (middle) extension rate, and (bottom) density for (left) STM2 and (right) STM4. Note the opposite long-term trends in calcification and extension rate between the two corals.

[22] Coral density of STM2 and STM4 showed no linear trend over the 43 years, despite considerable interannual and decadal variability (Figure 7). Subtracting the mean density for JFM from the mean density in the 12 JFM ENSO years revealed the ENSO density anomaly. The average density anomaly for each core during a positive ENSO year was different, with STM2 being positive and STM4 negative, yet the differences were statistically not significant (Table 4b and Figure 7).

[23] Calcification rates significantly declined over the 43 year period for coral STM2 while they significantly increased for STM4 (Figure 7). On interannual time scales, calcification rates were negatively correlated with Sr/Ca values in both corals, particularly since 1983 (Figure 7). Annual calcification rates of STM2 and STM4 were negatively correlated ($r^2 = 0.2$, $p < 0.001$). A highly significant negative correlation ($r^2 = 0.54$; $p < 0.001$) between ENSO-year calcification rates was also observed between the two corals (Figures 7 and S4).

[24] Annual average density, extension rate, and calcification were correlated with ERSST and HadISST for both STM2 and STM4. There were no significant correlations observed between the growth parameters of STM2 with either of the SST data. However, for STM4, significant positive correlations were observed between ERSST (not HadISST) with both extension rate ($r^2 = 0.13$, $p < 0.05$) and calcification rate ($r^2 = 0.09$, $p < 0.05$).

4. Discussion

4.1. Coral Sr/Ca Paleothermometry

[25] Various studies have found inconsistencies between long-term Sr/Ca records from coral colonies sampled close to one another [*Cahyarini et al.*, 2008; *Pfeiffer et al.*, 2009; *Cahyarini et al.*, 2011]. These differences are often attributed to local SST or environmental stress [*Marshall and McCulloch*, 2002; *Linsley et al.*, 2004; *DeLong et al.*, 2007]. However,

in cases where the relationship between coral Sr/Ca records cannot solely be explained by localized SST discrepancies, vital effects are considered the main contributor to inter-colony Sr/Ca variability [*Allison et al.*, 2001; *Cohen et al.*, 2001; *Cohen et al.*, 2002; *Allison and Finch*, 2004; *Sinclair*, 2005; *Sinclair et al.*, 2006; *Saenger et al.*, 2008; *Cohen and Gaetani*, 2010; *DeLong et al.*, 2011; *Gaetani et al.*, 2011; *Kuffner et al.*, 2012]. Here, two coral colonies sampled 0.72 km apart showed similar seasonal amplitudes in Sr/Ca, yet had different baseline averages, opposite long-term trends and displayed diverging interannual responses to ENSO anomalies. We believe such extreme Sr/Ca differences to be a result of growth-related vital effects, rather than local SST variability and/or environmental stress, as the two corals also displayed opposing growth characteristics.

[26] The regression slopes between max-min Sr/Ca and gridded SST data were −0.055 mmol/mol/°C and −0.064 mmol/mol/°C for STM2 and STM4, respectively. These values are close to the mean published Sr/Ca-SST response of −0.06 mmol/mol/°C [*Corrège*, 2006]. However, such values are lower than the expected Sr/Ca-SST relationship from abiogenic precipitation of aragonite (−0.038 mmol/mol/°C) [*Gaetani and Cohen*, 2006; *Cohen and Gaetani*, 2010; *Gaetani et al.*, 2011]. To equally assess Sr/Ca trends and interannual anomalies of both corals, we applied the mean published Sr/Ca-SST relationship of −0.06 mmol/mol/°C [*Corrège*, 2006].

4.2. Long-term SST Trends

[27] ERSST and HadISST displayed warming trends of different rates over the 43 year period, with ERSST increasing by 0.010°C yr^{-1} and HadISST by 0.002°C yr^{-1}. These differences are a result of the few observational data (ICOADS) available for the region, resulting in a weak consensus [*Kennedy et al.*, 2011; *Solomon and Newman*, 2012]. Corals STM2 and STM4 displayed diverging trends over the same 43 year period studied, with STM2 warming (negative Sr/Ca trend) by 0.023°C yr^{-1} and STM4 cooling (positive Sr/Ca trend) by 0.010°C yr^{-1}. Interestingly, the extension rates of both corals also differed, with STM2 showing a declining extension rate over the 43 years, and STM4 an increasing extension rate (Figure 6). The extension rate increase of STM4 was far greater (+0.018 cm yr^{-1}) than the decrease in extension rate of STM2 (−0.007 cm yr^{-1}; Figure 6). Assuming SST has increased over the 43 year period (at what rate remains unknown), it is likely that the two corals have responded differently to warming, causing STM2 to grow slower and STM4 to grow faster. Consequently, vital effects have likely influenced both STM2 and STM4 Sr/Ca values. This is particularly evident for STM4 given there was no significant annual average relationship observed with gridded SST.

[28] Differences in the extension rates (i.e., vital effect) of the two corals have influenced the skeletal Sr/Ca composition, causing diverging trends. According to *Cohen and Gaetani* [2010], as the rate of aragonite crystal growth increases, so does Sr/Ca. Given the increasing extension rate of STM4, this might account for the increase in skeletal Sr/Ca, resulting in an apparent cooling trend. Similarly, STM2 displayed a decreasing Sr/Ca trend giving an apparent warming trend; therefore, as its extension rate also decreased, the observed Sr/Ca trend may have been enhanced (towards more negative values/warming).

[29] As the extension rate increase of STM4 is far greater than the extension rate decrease of STM2 (+0.011 cm yr^{-1}; Figure 6), the difference between Sr/Ca trends should have been positive rather than negative (−0.039 mmol/mol over 43 years) if there was no temperature control on Sr/Ca. However, as the difference between Sr/Ca trends was negative, a warming trend has likely influenced both corals assuming a linear Sr/Ca-extension rate relationship. Differences between the Sr/Ca regression slopes of corals with SST are related to both the reliability of instrumental data and vital effect strength. As the difference in extension rates between the STM cores indicate that STM4 increased at a faster rate than STM2 decreased, we assume that the vital effect influence on the STM4 Sr/Ca trend was greater than STM2. This is one explanation as to why there was no observed relationship between annual mean gridded SST and STM4 Sr/Ca. This argument is augmented when comparing gridded SST with growth parameters of the two corals. SST data (ERSST only) showed significant correlations with STM4 extension rate and calcification rate, yet not with STM2. The influence of SST (assuming warming occurred) on STM4 growth must have therefore been greater than that on STM2, and vital effects stronger, overwhelming the Sr/Ca signal related to SST.

[30] The only annual mean Sr/Ca record to show a significant relationship with SST was STM2, where it negatively correlated with ERSST (not HadISST), albeit weakly. However, this significant correlation of annual mean ERSST and STM2 Sr/Ca was lost when both datasets were detrended. This suggests that the Sr/Ca-SST relationship was

largely related to the long-term trend rather than interannual variability. As the extension rate decrease of STM2 likely inflated the Sr/Ca warming trend, the question still remains whether the significant Sr/Ca-ERSST relationship would remain significant if extension rates did not vary over the 43 year period.

[31] In order to constrain the extent to which the declining extension rate (vital effect) of STM2 has enhanced its Sr/Ca trend, we can estimate a range in which SST has increased using the lower limit of other published slopes (−0.08 mmol/mol/°C) to take the maximum vital effects into consideration (assuming the −0.038 mmol/mol/°C slope of abiogenic aragonite precipitation represents no vital effects). As a result, the SST increase would equate to a lower limit of +0.75°C, which is higher than both SST datasets (+0.43°C and +0.09°C for ERSST and HadISST, respectively). For an upper limit, we use the regressed slope of the annual mean Sr/Ca relationship with ERSST (−0.056 mmol/mol/°C), which would equate to a rise of +1.07°C. This would suggest that SST off northeast Madagascar has risen by 0.75°C–1.07°C between 1963 and 2006. This value is significantly higher than the HadISST trend of +0.09°C, which *McClanahan et al.* [2009] used for satellite based coral mortality or ecological extinction prediction models [*Hoegh-Guldberg*, 1999; *Hughes et al.*, 2003; *Sheppard*, 2003]. An explanation as to why these warming trends are so different might be related to corals recording a local signal and HadISST recording a more regional signal. Alternatively, the uncertainties associated with gridded SST data may also explain the slow warming HadISST trend [*Kennedy et al.*, 2011]. However, given we have no long-term in situ data, we cannot verify this, complicating the assessment of SST trends inferred from corals.

[32] For the coral Sr/Ca composite record ($STM_{composite}$), the calculated 43 year trend of +0.30°C (range of 0.23–0.32°C using slopes of −0.08 and −0.056 mmol/mol/°C) lies between the ERSST and HadISST trends (yet closer to that of ERSST), and the standard deviation of $STM_{composite}$ was closer to that of HadISST and ERSST, compared to STM2 and STM4. If we assume that gridded data reflects the true SST trend at the reef scale, averaging of the two coral records indeed improves the long-term trend estimates, as suggested by *Pfeiffer et al.* [2009]. However, this is unlikely, and we cannot rule out that gridded SST underestimates long-term trends at the reef scale, and long-term SST trends in the SW IO are uncertain [*Kennedy et al.*, 2011; *Solomon and Newman*, 2012]. We believe the improved $STM_{composite}$ relationship observed with gridded data is likely a coincidence caused by the elimination of opposing trends between the two corals. We must therefore treat the composite record with caution and suggest a coincidental similarity with gridded SST data in terms of the long-term trend. Future studies dealing with Sr/Ca-based SST reconstructions should at least observe statistical relationships between records before compiling composite records.

4.3. ENSO Years

[33] To individually test the reliability of our three coral Sr/Ca records (STM2, STM4, and STMcomposite) in assessing large-scale climate teleconnection patterns such as ENSO, we correlated each record with global SST (Figure 8). Coral STM2 was the only records that revealed a spatial correlation pattern typical for Indo-Pacific SST teleconnections, whereas $STM_{composite}$ showed a weaker correlation and STM4 no correlation. This suggests that STM2 is a more reliable time series to assess large-scale teleconnections related to past ENSO variability than both STM4 and $STM_{composite}$.

[34] There were 12 recorded positive ENSO events over the 43 year period studied here (www.cpc.ncep.noaa.gov). Both ERSST and HadISST showed similar positive JFM anomalies that indicated an average warming of 0.22°C and 0.25°C, respectively, yet varied considerably for individual ENSO years (Table S1). For the same 12 ENSO years, the STM2 Sr/Ca anomalies (negative Sr/Ca) were in agreement with the gridded SST products and displayed positive temperature anomalies of similar magnitude, whereas STM4 displayed negative temperature anomalies, and $STM_{composite}$ only slightly positive (Table S1). Similar to the gridded data, Sr/Ca-based SST anomalies for individual years varied considerably. Standard deviations indicated that ENSO year JFM averages between the cores were statistically the same as the gridded SST anomalies (Table S1). However, statistically and on assessment of individual positive ENSO events (Table S1), STM2 showed reasonable agreement with instrumental SST data, whereas STM4 and $STM_{composite}$ did not (Tab. S1).

[35] Interestingly, calcification rates in STM2 and STM4 were opposite in their response to individual positive ENSO events (Figure S4). This also suggests a different growth response to ENSO SST anomalies, which may have modulated the coral Sr/Ca composition of either coral. According

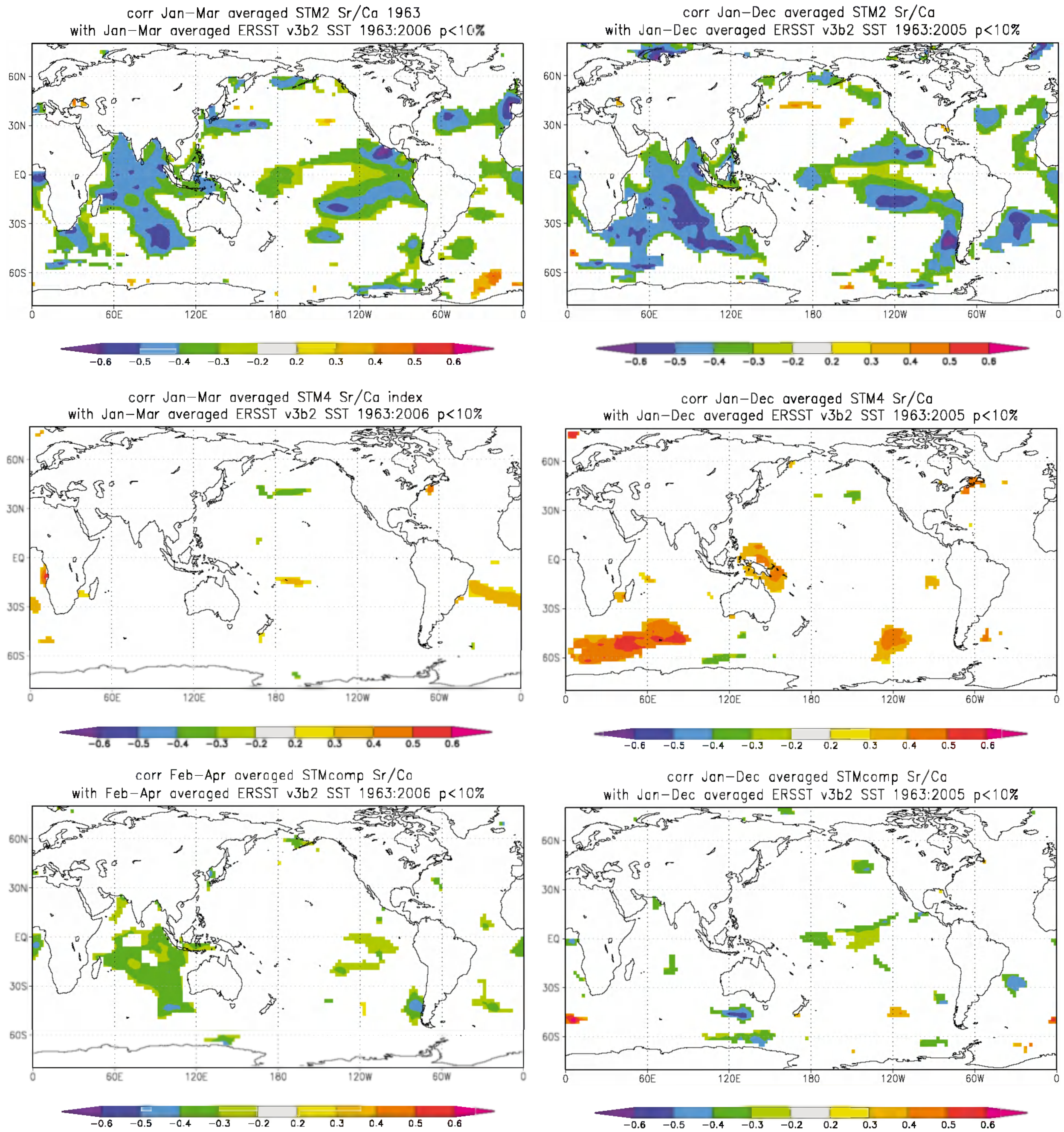

Figure 8. (Left) Spatial correlation of coral Sr/Ca with global SST for either the January to March or February to April period, (right) together with the annual means. Correlations are shown for (top) STM2, (middle) STM4, and (bottom) $STM_{composite}$, computed using the years 1963 to 2006. Only correlations significant above the 90% level are colored. Correlations were computed at http://climexp.knmi.nl/.

to *Cohen and Gaetani* [2010] and *Gaetani et al.* [2011], Rayleigh fractionation may cause Sr/Ca depletion as the mass of aragonite precipitated per "batch of calcifying fluid" increases. As there is an anomalous negative mean skeletal density and calcification response recorded by coral STM4 during a positive ENSO event, such Rayleigh fractionation would account for the anomalously higher mean skeletal Sr/Ca signal (Table 4). Similarly, as the mean density and calcification anomaly for STM2 is positive during a positive ENSO event, this would cause a negative mean Sr/Ca signal. In both cases, the mean Sr/Ca anomalies for corals STM2 and STM4 followed this pattern, suggesting densities and/or calcification rates may have modulated the skeletal Sr/Ca signal. This is in agreement with a recent mesocosm study by *Kuffner et al.* [2012]. They found that over a short nine month period, Sr/Ca was inversely related to calcification rate [*Kuffner et al.*, 2012].

[36] In order to constrain how much coral calcification has enhanced the STM2 ENSO anomalies, we can use the lower limit of other published slopes (−0.08 mmol/mol/°C) to take the maximum vital effects into consideration. As a result, the SST anomaly would equate to an approximate average increase of +0.17°C, which is lower than what both satellite datasets show (+0.22°C and +0.25°C for ERSST and HadISST, respectively). For an upper limit, we use the regressed slope of the annual mean Sr/Ca relationship with ERSST (−0.056 mmol/mol/°C), which would equate to an average positive anomaly of +0.25°C. This would suggest that positive ENSO events lead to an average SST increase of 0.17°C – 0.25°C off northeast Madagascar for the 12 ENSO years studied. However, given the large standard deviations involved, there was likely much variability between ENSO years, which is similarly observed in the gridded SST data. Therefore, the signal to noise ratio for 3 month averages in ENSO years is too low to faithfully record the SST amplitude of single events in eastern Madagascar.

4.4. Controls of Sr/Ca

[37] *Gaetani and Cohen* [2006], *Cohen and Gaetani* [2010] and *Gaetani et al.*, [2011] showed that coral Sr/Ca ratios are influenced by three processes/factors: (i) the mass fraction of aragonite precipitated by the coral (MFP), (ii) the crystal growth rate, and (iii) temperature. In this study, we find evidences suggesting that all three processes have influenced to some extent the two corals STM2 and STM4. (i) MFP and coral Sr/Ca are inversely correlated; therefore, the more efficient the coral is at precipitating aragonite from a batch of calcifying fluid, the lower the Sr/Ca ratio of the bulk aragonite will be. We draw similarities between this process and seasonal density/calcification changes in the two corals. (ii) As the growth rate of aragonite crystals increases, the Sr/Ca ratio of the crystals also increases. We observe this process in the two corals studied here, whereby differences in annual extension rates cause diverging Sr/Ca trends. The effects of (i) MFP and (ii) crystal growth rate are opposite, which we identify here. (iii) Finally, temperature also influences coral Sr/Ca (inversely), but the effect is relatively small compared to the other factors. Nevertheless, weak correlations of STM2 Sr/Ca and SST were identified, yet for STM4 not.

4.5. Inter-colony Sr/Ca Variability: Potential Causes

[38] Assuming the local physio-chemical conditions of the two corals were similar given the close proximity and full seawater exchange with the open ocean, other potential variables that may have influenced inter-colony Sr/Ca variability include (i) depth, (ii) age of the coral, and (iii) sampling off the optimal growth axis. (i) Depth, and in turn light intensity, may have influenced the growth response of coral STM4, as its apex was located 0.5 m higher than STM2 and therefore closer to the warmer wave-dominated surface. Increased extension rates are indeed linked to warmer SSTs and/or more optimal light levels [*Lough and Barnes*, 2000; *Reynaud et al.*, 2007]; however, this does not explain the declining extension rates observed in STM2. Also, it is unclear whether depth would cause the corals to respond differently to warmer ENSO years in terms of calcification. (ii) The age of the coral may also cause variability in the geochemical signals observed between corals, given STM4 is ca. twice the age of STM2 [*Marshall and McCulloch*, 2002]. However, it remains to be seen whether age can cause such divergent trends. (iii) If we sampled off the optimal growth axis for STM4, pre-1978, this may have caused more positive Sr/Ca values. However, the Sr/Ca-growth relationship remained similar both pre- and post-1978. It is also unlikely that errors introduced by age-model calculations would have caused the low correlations between cores, as clear cycles in Sr/Ca were observed (Figure 2) and corroborated against density and luminescence profiles [*Hendy and Gagan*, 2003; *Grove et al.*, 2010].

[39] As STM2 and STM4 were both drilled from the same coral species, *Porites lutea*, differences in growth responses may have been affected by the coral microbiology. It has been reported that some corals can shuffle or switch symbiont types in response to thermal stress events [*Berkelmans and van Oppen*, 2006] and that this may represent a means of adaptation to environmental change. Distinct symbiont genotypes are known to differ in their photosynthetic contribution to the coral host [*Loram et al.*, 2007], and calcification is thought to be a “photosynthesis-driven” process [*Colombo-Pallotta et al.*, 2010]. For instance, corals with the more heat tolerant symbiont type D are shown to

grow considerably slower (up to 38%) than corals with type C2 [*Cantin et al*., 2010; *Jones and Berkelmans*, 2010]. *Cohen et al*. [2002] proposed that algal symbionts affect the accuracy of the Sr/Ca thermometer in tropical coral species. Increased water temperature and increased symbiont activity are both thought to cause a simultaneous decrease in the Sr incorporation into the skeleton. This process is more dominant during summer calcification when symbiont activity is highest.

[40] Our results show that corals react differently to external forcing in terms of extension rate, density, and calcification [*Helmle et al*., 2011], which likely modulates the skeletal Sr/Ca composition. More specifically, *Porites* spp. have been shown to be particularly sensitive to thermal stress in terms of calcification [*Carricart-Ganivet et al*., 2012]. Corals STM2 and STM4 are good examples of how two colonies of the same species located less than 1 km apart can show opposite Sr/Ca trends and anomalies. Assuming some degree of warming occurred in the SW Indian Ocean between 1963 and 2006, warming trends are accompanied by an increasing extension rate of STM4 and a decrease in extension rate of STM2. This observation suggests high variability in coral growth between individual colonies in subtropical reef locations paired with relatively high SST seasonal cycles ($>5°C$). Consequently, interannual SST variations are of minor amplitude in comparison to seasonal changes. This in turn will complicate the coral based-SST reconstructions, especially interannual variability, due to vital effects likely increasing with increasing SST and growth variability. Although uncertain, the last 30 years have seen high rates of warming which can potentially enhance physiological stress for corals. This may have undermined the corals ability to faithfully record SST in the skeletal geochemistry; however, this assumption needs to be further tested at sites where reliable in situ SST observations exist.

5. Summary

[41] Coral vital effects modulate the precipitation of skeletal Sr/Ca, which can in turn affect its relationship with SST. Altering extension rates and densities in response to SST variability may overwhelm the Sr/Ca signal and in extreme circumstances produce opposing results. Here, we find two corals of the same species in the same environment with diverging growth responses to SST; yet, the influence of vital effects on Sr/Ca is consistent between corals. Increasing extension rates in STM4, over the 43 year period, were coupled with increasing Sr/Ca ratios, while decreasing extension rates in STM2 were coupled with decreasing Sr/Ca ratios. During individual positive ENSO events, calcification rates in STM4 and STM2 were negatively correlated, which may have modulated the Sr/Ca signals. It is therefore important to measure multiple cores to fully assess vital effects and their impact on Sr/Ca. Pooling records together can increase the reliability of reconstructions; however, in circumstances such as this, the coral composite record can be less reliable when two corals display such opposite signals. Whether the coral biology and/or local physiochemical environmental differences are the cause for Sr/Ca discrepancies between records, measuring growth parameters will assist in identifying and constraining them.

Acknowledgments

[42] This work was supported as part of the SINDOCOM grant under the Dutch NWO program “Climate Variability”, grant 854.00034/035. Additional support comes from the NWO ALW project CLIMATCH, grant 820.01.009, and the Western Indian Ocean Marine Science Association through the Marine Science for Management program under grant MASMA/CC/2010/02. We thank Karin Kissling for her assistance with the ICP-OES measurements at the University of Kiel, and Bob Koster and Rineke Gieles for their help with the UV-Core Scanner. Furthermore, we thank CAF/CORE Madagascar for granting the CITES permit, Bert Hoeksema from Naturalis and Brian Rosen and Nadia Santadomingo from the Natural History Museum in London for identifying the coral species, and Lars Reuning (RWTH Aachen, Germany), Juan D’Olivo Cordero (UWA Perth), Michael Holcomb (UWA Perth), and Delphine Dissard (UWA Perth) for fruitful discussions while writing this manuscript.

References

Alibert, C., and M. T. McCulloch (1997), Strontium/calcium ratios in modern *Porites* corals from the Great Barrier Reef as a proxy for sea surface temperature: calibration of the thermometer and monitoring of ENSO, *Paleoceanography*, *12*, 345–363.

Allison, N., and A. A. Finch (2004), High-resolution Sr/Ca records in modern Porites lobata corals: Effects of skeletal extension rate and architecture, *Geochem. Geophy. Geosyst.*, *5*, doi:10.1029/2004GC000696.

Allison, N. (1996), Geochemical anomalies in coral skeletons and their possible implications for palaeoenvironmental analyses, *Mar. Chem.*, *55*(3–4), 367–379.

Allison, N., A. A. Finch, S. R. Sutton, and M. Newville (2001), Strontium heterogeneity and speciation in coral aragonite: Implications for the strontium paleothermometer, *Geochim. Cosmochim. Ac.*, *65*, 2669–2676.

Annamalai, H., J. M. Slingo, K. R. Sperber, and K. Hodges (1999), The mean evolution and variability of the Asian summer monsoon: Comparison of the ECMWF and NCEP/NCAR reanalysis, *Monthly Weather Review*, *127*, 1157–1186.

Barnes, D. J., and R. B. Taylor (2005), On the nature and causes of luminescent lines and bands in coral skeletons: II. Contribution of skeletal crystals, *J. Exp. Mar. Biol. Ecol.*, *322*(2), 135–42.

Berkelmans, R., and M. J. H. van Oppen (2006), The role of zooxanthellae in the thermal tolerance of corals: A "nugget of hope" for coral reefs in an era of climate change, *P. R. Soc. B*, *273*, 2305–2312.

Cahyarini, S. Y., M. Pfeiffer, and W.-C. Dullo (2008), Improving SST reconstructions from coral Sr/Ca records: Multiple corals from Tahiti (French Polynesia), *Int. J. Earth Sci.*, doi:10.007/s00531-00008-00302-00532.

Cahyarini, S. Y., M. Pfeiffer, W.-C. Dullo, J. Zinke, S. Hetzinger, S. Kasper, C. Grove, and D. Garbe-Schonberg (2011), Comment on "A snapshot of climate variability at Tahiti at 9.5 ka using a fossil coral from IODP Expedition 310" by Kristine L. DeLong, Terrence M. Quinn, Chuan-Chou Shen, and Ke Lin, *Geochem. Geophy. Geosy.*, *12*, Q03012.

Cantin, N. E., A. L. Cohen, K. B. Karnauskas, A. M. Tarrant, and D. C. McCorkle (2010), Ocean warming slows growth in the central Red Sea, *Science*, *329*(5989), 322–325.

Carricart-Ganivet, J. P., J. M. Lough, and D. J. Barnes (2007), Growth and luminescence characteristics in skeletons of massive *Porites* from a depth gradient in the central Great Barrier Reef, *J. Exp. Mar. Biol. Ecol.*, *351*, 27–36.

Carricart-Ganivet, J. P., N. Cabanillas-Terán, I. Cruz-Ortega, and P. Blanchon (2012), Sensitivity of calcification to thermal stress varies among genera of massive reef-building corals, *PLoS One*, *7*(3), e32859, doi:10.1371/journal.pone.0032859.

Cohen, A. L., and G. A. Gaetani (2010), Ion partitioning and the geochemistry of coral skeletons: Solving the mystery of the vital effect, *EMU Notes in Mineralogy*, *11*, 377–397.

Cohen, A. L., G. D. Layne, S. R. Hart, and P. S. Lobel (2001), Kinetic controls of skeletal Sr/Ca in a symbiotic coral: Implications for the paleotemperature proxy, *Paleoceanography*, *16*, 20–26.

Cohen, A. L., K. E. Owens, G. D. Layne, and N. Shimizu (2002), The effect of algal symbionts on the accuracy of Sr/Ca paleotemperatures from coral, *Science*, *296*, 331–333.

Colombo-Pallotta, M. F., A. Rodríguez-Román, and R. Iglesias-Prieto (2010), Calcification in bleached and unbleached *Montastraea faveolata*: Evaluating the role of oxygen and glycerol, *Coral Reefs*, *29*(4), 899–907.

Corrège, T. (2006), Sea surface temperature and salinity reconstructions from coral geochemical tracers, *Palaeogeogr. Palaeoclimatol. Palaeoecol.*, *232*, 408–428.

DeLong, K. L., T. M. Quinn, and F. W. Taylor (2007), Reconstructing twentieth-century sea surface temperature variability in the southwest Pacific: A replication study using multiple coral Sr/Ca records from New Caledonia, *Paleoceanography*, *22*, PA4212, doi:10.1029/2007PA001444.

DeLong, K. L., J. Flannery, C. R. Maupin, R. Z. Poore, and T. M. Quinn (2011), A coral Sr/Ca calibration and replication study of two massive corals from the Gulf of Mexico, *Palaeogeogr. Palaeoclimatol. Palaeoecol.*, *307*, 117–128, doi:10.1016/j.palaeo.2011.05.005.

Felis, T., and J. Pätzold (2003), Climate records from corals, in *Marine Science Frontiers for Europe*, edited by G. Wefer, F. Lamy and F. Mantoura, pp. 11–27, Spinger, Berlin, Heidelberg, New York, Tokyo.

Ferrier-Pages, C., F. Boisson, D. Allemand, and E. Tambutte (2002), Kinetics of strontium uptake in the scleractinian coral Stylophora pistillata, *Mar. Ecol. Prog. Ser.*, *245*, 93–100.

Gaetani, G. A., and A. L. Cohen (2006), Element partitioning during precipitation of aragonite from seawater: A framework for understanding paleoproxies, *Geochim. Cosmochim. Acta*, *70*, 4617–4634.

Gaetani, G. A., A. L. Cohen, Z. Wang, and J. Crusius (2011), Rayleigh-based, multi-element coral thermometry: A biomineralization approach to developing climate proxies, *Geochim. Cosmochim. Acta*, *75*, 1920–1932.

Grove, C. A., R. Nagtegaal, J. Zinke, T. Scheufen, B. Koster, S. Kasper, M. T. McCulloch, G. van den Berg, and G.-J. A. Brummer (2010), River runoff reconstructions from novel spectral luminescence scanning of massive coral skeletons, *Coral Reefs*, *29*, 579–591.

Hart, S. R., and A. L. Cohen (1996), An ion probe study of annual cycles of Sr/Ca and othet trace elements in corals, *Geochim. Cosmochim. Acta*, *60*, 3075–3084.

Helmle, K. P., K. E. Kohler, and R. E. Dodge (2002), Relative optical densitometry and the coral X-radiograph densitometry system: CoralXDS, Presented Poster, *Int. Soc. Reef Studies 2002 European Meeting*. Cambridge, England. Sept. 4–7.

Helmle, K. P., R. E. Dodge, P. K. Swart, D. K. Gledhill, and C. M. Eakin (2011), Growth rates of Florida corals from 1937 to 1996 and their response to climate change, *Nat. Commun.*, *2*, doi:0.1038/ncomms1222.

Hendy, E. J., and M. K. Gagan (2003), Chronological control of coral records using luminescent lines and evidence for non-stationary ENSO teleconnections in northeast Australia, *The Holocene*, *13*, 187–199.

Hoegh-Guldberg, O. (1999), Climate change, coral bleaching and the future of the world's coral reefs, *Mar. Freshwater Res.*, *50*, 839–866.

Hughes, T. P., et al. (2003), Climate change, human impacts, and the resilience of coral reefs, *Science*, *301*, 929–933.

Inoue, M., M. Nohara, T. Okai, A. Suzuki, and H. Kawahata (2004), Concentrations of trace elements in carbonate reference materials coral JCp-1 and giant clam JCt-1 by inductively coupled plasma-mass spectrometry, *Geostan. Geoanal. Res.*, *28*(3), 411–416.

Jones, A., and R. Berkelmans (2010), Potential costs of acclimatization to a warmer climate: Growth of a reef coral with heat tolerant vs. sensitive symbiont types, *PLoS One*, *5*, doi:10.1371/jounal.pone.0010437.t005.

Kennedy, J. J., N. A. Rayner, R. O. Smith, D. E. Parker, and M. Saunby (2011), Reassessing biases and other uncertainties in sea surface temperature observations measured in situ since 1850: 1. Measurement and sampling uncertainties, *J. Geophys. Res.*, *116*, D14103, doi:10.1029/2010JD015218.

Kuffner, I. B., P. L. Jokiel, K. S. Rodgers, A. J. Andersson, and F. T. Mackenzie (2012), An apparent "vital effect" of calcification rate on the Sr/Ca temperature proxy in the reef coral Montipora capitata, *Geochem. Geophys. Geosyst.*, *13*, Q08004, doi:10.1029/2012GC004128.

Linsley, B. K., G. M. Wellington, D. P. Schrag, L. Ren, M. J. Salinger, and A. W. Tudhope (2004), Geochemical evidence from corals for changes in the amplitude and spatia; Pattern of South pacific interdecadal climate variability over the last 300 years, *Clim. Dynam.*, *22*, 1–11.

Linsley, B. K., A. Kaplan, Y. Gouriou, J. Salinger, P. B. deMenocal, G. M. Wellington, and S. S. Howe (2006), Tracking the extent of the South Pacific Convergence Zone since the early 1600s, *Geochem. Geophys. Geosyst.*, *7*, doi:10.1029/2005GC00115.

Loram, J. E., H. G. Trapido-Rosenthal, and A. E. Douglas (2007), Functional significance of genetically different symbiotic algae *Symbiodinium* in a coral reef symbiosis, *Mol. Ecol.*, *16*, 4849–4857, doi:10.1111/j.1365-294X.2007.03491.x.

Lough, J. M., and D. J. Barnes (2000), Environmental controls on growth of the massive coral Porites, *J. Exp. Mar. Biol. Ecol.*, *245*, 225–243.
Marshall, J. F., and M. T. McCulloch (2002), An assessment of the Sr/Ca ratio in shallow water hermatypic corals as a proxy for sea surface temperature, *Geochim. Cosmochim. Acta*, *66*, 3263–3280.
McClanahan, T. R., M. Ateweberhan, J. Omukoto, and L. Pearson (2009), Recent seawater temperature histories, status, and predictions for Madagascar's coral reefs, *Mar. Ecol. Prog. Ser.*, *380*, 117–128.
Paillard, D., L. Labeyrie, and P. Yiou (1996), Macintosh program performs time series analysis. *Eos Transactions AGU*, *77*, 379.
Pfeiffer, M., W.-C. Dullo, J. Zinke, and D. Garbe-Schönberg (2009), Three monthly coral Sr/Ca records from the Chagos Archipelago covering the period of 1950–1995 A.D.: Reproducibility and implications for quantitative reconstructions of sea surface temperature variations, *Int. J. Earth Sci.*, *98*, doi:10.007/s00531-008-0326-z.
Quinn, T. M., F. W. Taylor, and T. J. Crowley (2006), Coral-based climate variability in the Western Pacific Warm Pool since 1867, *J. Geophys. Res.*, *111*, C11006, doi:10.1029/2005JC003243.
Rayner, N. A., D. E. Parker, E. B. Horton, C. K. Folland, L. V. Alexander, D. P. Rowell, E. C. Kent, and A. Kaplan (2003), Global analyses of sea surface temperature, sea ice, and night marine air temperature since the late nineteenth century, *J. Geophys. Res.*, *108*, doi:10.1029/2002JD002670.
Reynaud, S., C. Ferrier-Pages, A. Meibom, S. Mostefaoui, R. Mortlock, R. Fairbanks, and D. Allemand (2007), Light and temperature effects on Sr/Ca and Mg/Ca ratios in the scleractinian coral Acropora sp., *Geochim. Cosmochim. Acta*, *71*, 354–362.
Reynolds, R. W., N. A. Rayner, T. M. Smith, D. C. Stokes, and W. Q. Wang (2002), An improved in situ and satellite SST analysis for climate, *J. Climate*, *15*, 1609–1625.
Saenger, C., A. L. Cohen, D. W. Oppo, and D. Hubbard (2008), Interpreting sea surface temperature from strontium/calcium ratios in *Montastrea* corals: Link with growth rate and implications for proxy reconstructions, *Paleoceanography*, *23*, PA3102, doi:10.1029/2007PA001572.
Schott, F. A., S.-P. Xie, and J. P. McCreary Jr. (2009), Indian Ocean circulation and climate variability, *Rev. Geophys.*, *47*, RG1002, 1–46.
Schrag, D. (1999), Rapid analysis of high-precision Sr/Ca ratios in corals and other marine carbonates, *Paleoceanography*, *14*(2), 97–102.
Sinclair, D.J. (2005), Correlated trace element "vital effects" in tropical corals: A new geochemical tool for probing biomineralization, *Geochim. Cosmochim. Acta*, *69*, 3265–3284.
Sinclair, D. J., B. Williams, and M. Risk (2006), A biological origin for climate signals in corals - Trace element "vital effects" are ubiquitous in Scleractinian coral skeletons, *Geophys. Res. Lett.*, *33*, doi:10.1029/2006GL027183.
Sheppard, C. (2003), Predicted recurrences of mass coral mortality in the Indian Ocean, *Nature*, *425*, 294–297.
Smith, T. M., and R. W. Reynolds (2004), Improved Extended Reconstruction of SST (1854–1997), *J. Climate*, *17*, 2466–2477.
Solomon, A., and M. Newman (2012), Reconciling disparate twentieth-century Indo-Pacific ocean temperature trends in the instrumental record, *Nature Clim. Change*, *2*, 691–699.
Storz, D., and E. Gischler (2011), Coral extension rates in the NW Indian Ocean I: Reconstruction of 20th century SST variability and monsoon current strength, *Geo-Mar. Lett.*, *31*, 141–154.
de Villiers, S., G. T. Shen, and B. K. Nelson (1994), The Sr/Ca-temperature relationship in coralline aragonite: Influence of variability in (Sr/Ca)seawater and skeletal growth parameters, *Geochim. Cosmochim. Acta*, *58*, 197–208.
de Villiers, S., M. Greaves, and H. Elderfield (2002), An intensity ratio calibration method for the accurate determination of Mg/Ca and Sr/Ca of marine carbonates by ICP-AES, *Geochem. Geophys. Geosyst.*, *3*(1), 1001.
Woodruff, S. D., H. F. Diaz, S. J. Worley, R. W. Reynolds, and S. J. Lubker (2005), Early ship observational data and ICOADS, *Clim. Chang.*, *73*, 169–194.